



저작자표시-비영리-변경금지 2.0 대한민국

이용자는 아래의 조건을 따르는 경우에 한하여 자유롭게

- 이 저작물을 복제, 배포, 전송, 전시, 공연 및 방송할 수 있습니다.

다음과 같은 조건을 따라야 합니다:



저작자표시. 귀하는 원저작자를 표시하여야 합니다.



비영리. 귀하는 이 저작물을 영리 목적으로 이용할 수 없습니다.



변경금지. 귀하는 이 저작물을 개작, 변형 또는 가공할 수 없습니다.

- 귀하는, 이 저작물의 재이용이나 배포의 경우, 이 저작물에 적용된 이용허락조건을 명확하게 나타내어야 합니다.
- 저작권자로부터 별도의 허가를 받으면 이러한 조건들은 적용되지 않습니다.

저작권법에 따른 이용자의 권리는 위의 내용에 의하여 영향을 받지 않습니다.

이것은 [이용허락규약\(Legal Code\)](#)을 이해하기 쉽게 요약한 것입니다.

[Disclaimer](#)

약학석사 학위논문

**Validation of interactions between
aminoacyl-tRNA synthetases and
cancer-associated factors using
FRET-based screening system**

FRET 기반의 screening system 을 사용한
aminoacyl-tRNA synthetases 와
cancer-associated factors 의 상호작용 검증

2013 년 2 월

서울대학교 융합과학기술대학원
분자의학 및 바이오제약학과 의약생명과학전공
박 보 라 진 아

**Validation of interactions between aminoacyl-
tRNA synthetases and cancer-associated
factors using FRET-based screening system**

**FRET 기반의 screening system 을 사용한 aminoacyl-
tRNA synthetases 와 cancer-associated factors 의
상호작용 검증**

지도 교수 김 성 훈

이 논문을 약학석사 학위논문으로 제출함

2012년 10월

서울대학교 융합과학기술대학원
분자의학 및 바이오제약학과 의약생명과학 전공
박 보 라 진 아

박보라진아의 약학석사 학위논문을 인준함

2013년 1월

위 원 장 _____ (인)

부 위 원 장 _____ (인)

위 원 _____ (인)

ABSTRACT

Aminoacyl-tRNA synthetases(ARSs) are essential proteins that are involved in cellular protein synthesis and viability. They catalyse the specific amino acids to their cognate tRNAs with a high fidelity. However, previous study shows that these enzymes are multi-functional proteins that are involved in diverse cellular processes. According to the recent study, a systematic analysis of the expression of ARSs indicates that these proteins are associated with cancer. Because of the need to identify the correlation, we developed a cell-based high throughput screen method using Förster resonance energy transfer (FRET) for anticancer activity in the living cells. Fluorescence resonance energy transfer (FRET) is unique in generating fluorescence signals that are sensitive to molecular conformation, association, and separation in the 1-10nm range. At first, we constructed vectors that expressed cyan fluorescent protein (CFP) tagged ARSs and yellow fluorescent protein (YFP) tagged CAGs. Then we used a confocal microscope and calculated the FRET efficiency. As a result, we found that AIMP3 and RPSA protein pair which has higher FRET efficiency than the control. To confirm this protein-protein

interaction, we conducted co-immunoprecipitation and in vitro pull down assay. From the previous experiments, we identified that the AIMP3 and RPSA has a direct interaction.

Accordingly, our results indicated that FRET-based validating system could be used to detect protein-protein interactions. Moreover, with our assay, it could help with the development of new anti-cancer drugs in the future.

Key words: Aminoacyl-tRNA synthetases (ARSs), Cancer-associated genes (CAGs), protein-protein interaction, Fluorescence resonance energy transfer (FRET), anti-cancer drug target

Student ID: 2011-23058

CONTENTS

ABSTRACT	1
CONTENTS	3
LIST OF FIGURES	5
LIST OF TABLES	6
I. INTRODUCTION	7
II. MATERIALS AND METHODS	10
1. Vector construction	10
2. Cell culture	11
3. DNA transfection	11
4. FRET assay	12
5. Co-immunoprecipitation and western blot analysis	12
_____	12

6. GST fusion protein purification and in vitro pull-down assay	13
III. RESULT	15
1. Development of the optimized donor and acceptor pairs for FRET screening	15
2. Monitoring FRET signals in living mammalian cells	16
3. Validation of the FRET screening results	18
4. The improper orientation of AIMP3-CFP/RPSA-YFP indicates no FRET	19
5. The aspects of expression to consider for FRET occurrence	20
IV. DISCUSSION	32
V. REFERENCE	34
VI. 국문초록	37

LIST OF FIGURES

Figure1. Schematic diagrams and possible permutation between ARS and CAGs	21
Figure2. AIMP3-CFP & RPSA-YFP pair was positive result by the FRET screening	24
Figure3. The comparison of the FRET screening results between the positive control and negative control	26
Figure4. AIMP3 physically interacts with RPSA	28
Figure5. AIMP3 and RPSA must have the appropriate relative orientation to transfer the energy	29
Figure6. Molecules must be in close proximity on a nanometer (10^{-9} m) scale	30

LIST OF TABLES

Table1. Lists of constructed plasmids for FRET pairs_____22

**Table2. Lists of primer sequences of metastasis related cancer-
associated genes_____23**

INTRODUCTION

Aminoacyl-tRNA synthetases(ARSs) are essential proteins that are involved in cellular protein synthesis and viability. They catalyse the specific amino acids to their cognate tRNAs with a high fidelity. However, previous study shows that these enzymes are multi-functional proteins that are involved in diverse cellular processes, such as tRNA processing, RNA splicing and trafficking, rRNA synthesis, apoptosis, angiogenesis, inflammation and tumorigenesis [1, 2]. According to the recent study, a systematic analysis of the expression of ARSs indicates that these proteins are associated with cancer. The links between ARSs and 123 first neighbor cancer-associated genes were identified and suggested as a network model that displays how the ARSs and AIMP3 could be functionally linked to each other in different biological pathways. Although those data do not show any specific connection of ARSs to biological processes or cancers, the connection imply that they have specific roles in tumorigenesis [3]. Several ARSs are secreted or released from diverse cellular sources under physiological conditions according to previous study. Although further investigation is needed to understand some of the

secreted ARSs are involved in metastasis [3]. Therefore we focused CAGs specifically related with metastasis, and established the correlation between ARSs and CAGs.

To identify the correlation, we developed a cell-based high throughput screen method using Förster resonance energy transfer (FRET) for anticancer activity in the living cells. FRET can be used to detect changes in protein conformations or protein-protein interactions. The FRET efficiency is considered by the distance and relative orientation of the two fluorophores, because it is observed when two fluorophores in distances less than 10nm [4]. Developers are forced to spend large amounts of time by trial and error because both distance and relative orientation are hard to predict [5]. Therefore, FRET is highly relevant for biochemical reactions, such as protein-protein or protein-DNA interactions. FRET could analysis molecular interactions by a sensitive fluorescence read-out [6]. Not surprisingly, FRET has developed into a widely used tool in cell biology, biophysics and biomedical imaging with very high temporal resolution [7, 8]. We choose the sensitized emission method among a lot of developed FRET methods. The concept is to use two kinds of different filters combining with samples in such a way that the donor is excited by a specific wavelength of light, and the

signal is collected by using emission filters chosen for the donor fluorescence and the acceptor fluorescence. This allows the researcher to subtract the bleed-through from the both excitation and emission [9].

FRET is highly sensitive and subjective, thus we chose the optimal fluorescent protein pair used in previous study [10] [11]. The pZsYellow vector encodes a yellow fluorescent protein, ZsYellow, derived from human codon-optimized variant of wild-type *Zoanthus* sp. and pAmCyan encodes a cyan fluorescent protein, AmCyan, derived from human codon-optimized variant of wild-type *Anemonia majano*. Two fluorescent proteins, AmCyan and ZsYellow, have appropriate fluorescence excitation and emission properties for the measurement of close molecular distance [12]. When these two molecules are positioned within ~10nm of each other, energy can transfer from the excited state of the CFP fluorophore to the unoccupied excited state of the YFP fluorophore [13].

MATERIALS AND METHODS

Vector construction

The cDNAs of the CAGs were purchased from Clontech, and inserted into the YFP expression vectors pZsYellow-N1. The cDNAs of the ARSs are amplified by PCR, and inserted into pAmCyan-N1 or -C1 vectors. The both of plasmids expressing the CFP (pAmCyan-N1,-C1) and YFP (pZsYellow-N1,-C1) were purchased from Clontech. As seen from table 1 and table 2, the sixteen ARSs were amplified by PCR and subcloned into the pAmCyan-N1,-C1 vectors. The AIMP3 of the ARSs was constructed to pZsYellow-N1 for using the positive control. To generate the positive control, Xho1-Sal1 digested plasmid encoding YFP was ligated to pAmCyan-N1 vectors, which encodes the CFP –YFP fusion protein linked by a short peptide (8 amino acids in length). The ten metastasis related CAGs were tagged with YFP in the same way.

Cell culture

CHO-K1 cells were maintained in RPMI medium (with 2.05mM L-Glutamine, Hyclone) with 10% fetal bovine serum (FBS, Hyclone) and 50 µg/ml penicillin and streptomycin at 37°C in a 5% CO₂ incubator. HEK 293T cells were cultured in DMEM medium (with 4.00mM L-Glutamine, 4500mg/L Glucose and Sodium Pyruvate, Hyclone) supplemented with 10% fetal bovine serum (FBS, Hyclone) and 50 µg/ml penicillin and streptomycin at 37°C in a 5% CO₂ incubator.

DNA transfection

Transfections with DNA were performed by suggested protocol using Lipofectamine 2000 (Invitrogen). CHO-K1 cells were seeded in a 12-well culture plate (10⁵ cells/2 ml/well) in one day before transfection, and then the ARSs-CFP/CAGs-YFP complex (totally 2µg of DNA) was treated into cells and incubated in the culture medium without FBS for 3 hours at 37°C. Replace the transfection mixture 3 hours later with complete media, and analyze transgene expression 24 hours later.

FRET assay

CHO-K1 cells cultured on coverslips were fixed with 4% paraformaldehyde at 25°C for 10min and washed twice with PBS. Images were visualized under an AIRsi confocal microscope (Nikon), and processed using the NIS-element software (Nikon). All FRET observations were performed after cells were transfected for 24 hour [14]. The donor (CFP) was excited at 457nm, and its fluorescence was detected in a wavelength of 464~499nm (CFP channel), whereas the excitation at 514nm and the emission at 525~555nm were used for detecting the acceptor (YFP) (YFP channel). FRET was detected at the excitation of 457nm and the emission of 525~555nm (FRET channel). Fluorescence images of the transfected cells were taken at the CFP-, YFP- and FRET channels sequentially at a resolution of 512×512. The FRET efficiency was calculated using the FRET module in the NIS-element software. The Calculated FRET efficiency was obtained more than 10 cells for each pair.

Co-immunoprecipitation and western blot analysis

CHO-K1 cells were washed twice with PBS, and lysed with lysis buffer (50mM Tris-HCl (pH 7.4), 150mM NaCl, 0.5% Triton X-100, 5mM EDTA, 10% glycerol and protease inhibitor (Calbiocam)). The protein extracts were incubated with normal IgG as control, GFP- and Flag antibody for 4 hour at 4 °C with agitation. Protein G agarose was added to protein-antibody complex for 16 hour. After washing four times with the cold lysis buffer, the precipitates were dissolved in the SDS sample buffer and separated by SDS-PAGE. Anti-YFP antibody and Anti-FLAG antibody were used for western blotting. Antibody to CFP and YFP was purchased from Clontech (Anti-RCFP polyclonal pan antibody, #632475). The antibody was diluted 1:1000 for westernblotting. Antibody to Flag was purchased from Sigma (#F3165).

GST fusion protein purification and *in vitro* pull-down assay

GST-AIMP3 fusion protein and GST protein were purified as follows. AIMP3 cloned into the pGEX-4T1 vector that expressed GST protein. GST and GST-AIMP3 were transformed into BL21(DE3) strain competent cells

and cultured in LB media for overnight. Proteins were induced by adding 0.5mM isopropyl- β -D-thiogalactopyranoside (IPTG) and incubated at 28°C for 6 hours. Harvested cells, centrifuged at 4000rpm for 15 minutes, were lysed by sonication with lysis buffer (cold PBS containing 5% glycerol). Lysed cells were centrifuged at 10,000rpm, 4°C, for 30 minutes. The supernatant was incubated with glutathione sepharose 4B (GE healthcare) at 4°C for 6 hours. The beads were washed three times with lysis buffer. To check the purity and quantity of GST-fusion protein, eluted proteins were separated by SDS-PAGE and detected by coomassie blue staining.

RESULTS

Development of the optimized donor and acceptor pairs for FRET screening

We first optimized the donor and acceptor fluorescent proteins. In the previous FRET study, the CFP and YFP variants are mostly used as the donor and the acceptor, respectively [11]. Therefore we will choose CFP and YFP as the donor and the acceptor. Each of the sixteen ARSs was subcloned to CFP and ten metastasis related CAGs were tagged with YFP (Figure 1A). To verification that these fluorescent proteins were practicable, cells were transfected with plasmids encoding ARSs-CFP or CAGs-YFP respectively, and co-transfected with ARSs-CFP/CAGs-YFP pairs. A cyan and yellow fluorescent proteins (CFP and YFP) serving as a donor and an acceptor, respectively, were analyzed using the FRET efficiency to monitor the interaction between those two proteins. Furthermore, we used a FRET construct consisting of a CFP-YFP fusion protein (Figure 1B). The two fluorescent proteins are connected by a short linker of eight amino acids. Such

a donor-acceptor fusion can also serve as a good positive control for FRET, because of the proximity of the CFP and YFP fluorophores held together by the linker peptide.

Monitoring FRET signals in living mammalian cells

Detection of FRET between cyan and yellow fluorescent proteins is a key method for quantifying protein-protein interactions inside living cells. If dimerization of CFP-and YFP-tagged protein resulted in energy transfer, we would expect that these proteins had interaction each other. To examine the constructed FRET pairs, cells were cotransfected with CFP and YFP and quantified by the laser scanning confocal microscope.

From the screening, we identified only one FRET pairs that has increased the FRET efficiency ratio relative to positive control pair. AS a first approximation the average signal was computed in FRET mode, for both, the donor only, acceptor only and the FRET sample (Figure 2A). In this report, we applied confocal microscopy to quantify FRET using a sensitized emission FRET method that is the simplest method for monitoring FRET as described

earlier. The simultaneously measured intensities of the donor and acceptor can be used for the ratiometric detection of FRET by using two-channel filters for the donor fluorescence and the acceptor fluorescence [8, 9]. The Different filter combinations is used with samples that contain only the donor, only the acceptor, or the FRET sample with both the donor and acceptor. This allows to determine the amount of cross-talk between excitation and emission and to compensate the bleed-through from the FRET measurement [15]. The reference spectral images of the fluorescent proteins were previously collected from cells overexpressing the only CFP or YFP tagged proteins, respectively (Figure 2B). Simply put, the donor only sample consists of the same cells transfected with CFP only. The FRET efficiency was calculated for each pixel in the images (see Materials and methods), and the spatial FRET distribution was depicted using discrete pseudocolors (Figure 2A, the rightmost one). The calculated energy transfer efficiency for positive control was identical with an average value of 16% (Figure 2C & 3A). In this work, we used the two kinds of pairs as the positive control. First, the CFP-YFP fusion protein was established experimental control based on previous FRET papers. Second, MRS-CFP/AIMP3-YFP pairs also used as positive because of MRS and AIMP3 has known to interact each other directly from the recent study [16].

The calculated FRET efficiency of AIMP3-CFP/RPSA-YFP pairs was approximately two-fold higher than positive control. We interpret this spatial distribution of the high FRET efficiencies as reflecting those two proteins interact in close distance, not by coincidence.

In the previous study, KRS binds to RPSA protein directly upon treating laminin [17]. Thus, without laminin treatment, no FRET was observed in KRS-CFP/RPSA-YFP pair. Therefore, these pair was used as a negative control in these preparations (Figure 3C). This result indicates that the FRET observation needs to coordinate the additive signal in these cells.

Validation of the FRET screening results

To verify the potency of that selected FRET pairs from the initial screening, we examined that AIMP3 would bind to RPSA in biochemical approach. RPSA was synthesized *in vitro* and subjected to pull-down with GST and GST-AIMP3. RPSA co-precipitated with GST-AIMP3 weakly when it exposed in a short time. Afterwards, immunoblotting using the anti-YFP antibody showed that AIMP3-FLAG was specifically co-precipitated with

RPSA-YFP but not with IgG (Figure 4B). Thus, AIMP3 physically interacts with RPSA, which correspond with the result of FRET screening.

The improper orientation of AIMP3-CFP/RPSA-YFP indicates no FRET

The FRET efficiency is known to dependent primarily on both the distance and the relative orientation of the donor and the acceptor [18]. The cellular stoichiometry of the donor and acceptor can be variable for intermolecular FRET studies [15]. In consequence, we monitored the FRET efficiency measured from cells co-expressing AIMP3-CFP and RPSA-YFP with variable orientations. We found a clear correlation between the FRET efficiency value and the donor/acceptor stoichiometry (Figure 5). As described in above, the different orientations of the AIMP3-CFP and RPSA-YFP indicate a conflicting result in FRET efficiencies.

The aspects of expression to consider for FRET occurrence

Two fluorescent proteins should have close molecular distances to measure fluorescence excitation and emission spectrum. These two molecules are positioned within ~10nm of each other so that energy can transfer from the donor fluorophore to acceptor fluorophore. HRS-CFP and CD44-YFP identically expressed in the cytosol of the cells (Figure 6A). In contrast, MRS-CFP and MYC-YFP pair had shown the different aspects of expression (Figure 6B). Because of the individual proteins in cells have own expression patterns for various reason, all ARSs and CAGs did not have the same aspects of protein expression.

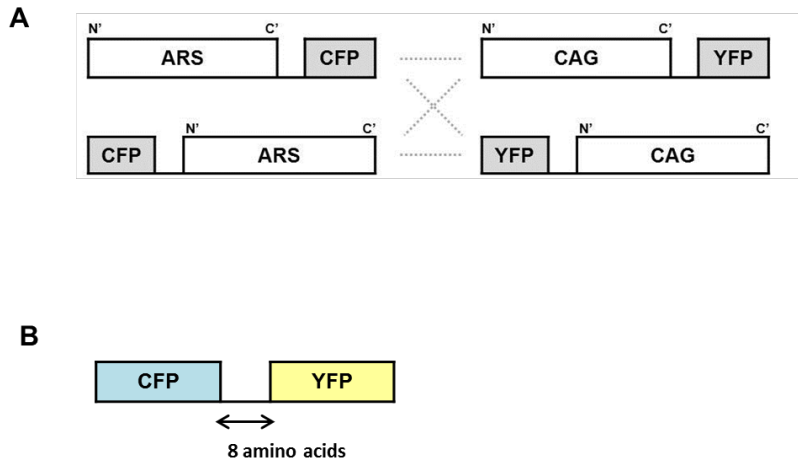


Figure1. Schematic diagrams and possible permutation between ARS and CAGs

A cyan and yellow fluorescent proteins (CFP and YFP) serving as a donor and an acceptor, respectively. (A) CFP(pAmCyan), a cyan fluorescent protein used as a FRET donor; YFP(pZsYellow), a yellow fluorescent protein used as a FRET acceptor. ARSs were subcloned to CFP and CAGs were tagged with YFP. The following four combinations are feasible; ARS-CFP (N') /CAG-YFP (N') , ARS-CFP (N')/ CAG-YFP (C') ARS-CFP (C')/ CAG-YFP (C') , ARS-CFP (C')/ CAG-YFP (N'). (B) A vector, pAmCyan-pZsYellow, which encodes the CFP –YFP fusion protein linked by a short peptide (8 amino acids in length) was generated and used as positive control.

A

	Insert gene	Target vector
AIMPs	AIMP1	pAmCyan-C1
	AIMP2	pAmCyan-N1
	AIMP2-DX2	pAmCyan-N1
	AIMP3	pAmCyan-N1
	AIMP3	pAmCyan-C1
	AIMP3	pZsYellow-N1
ARSs	AlaRS	pAmCyan-N1
	FRSa	pAmCyan-N1
	FRSb	pAmCyan-N1
	GRS	pAmCyan-C1
	HRS	pAmCyan-N1
	KRS	pAmCyan-C1
	MRS	pAmCyan-N1
	MRS	pAmCyan-C1
	NRS	pAmCyan-N1
	QRS	pAmCyan-N1
SRS	pAmCyan-N1	

B

	Insert gene	Target vector
CAGs (Metastasis)	CD44	pZsYellow-N1
	CLTC	pZsYellow-N1
	GPHN	pZsYellow-N1
	ICAM1	pZsYellow-N1
	ILK	pZsYellow-N1
	IQGAP1	pZsYellow-N1
	MCC	pZsYellow-N1
	RPSA	pZsYellow-N1
	RPSA	pZsYellow-C1
	SFTPb	pZsYellow-N1

Table1. Lists of constructed plasmids for FRET pairs

(A) The list of the ARSs-CFP. (B) The list of CAGs-YFP related metastasis field. Each of the 16 ARSs were subcloned to CFP and 10 metastasis related CAGs were tagged with YFP. Only the AIMP3 of the ARSs was constructed to YFP for the positive control.

Gene	Restriction enzyme	Primer sequence
CD44	XhoI-F	ccg ctcgag ATG GAC AAG TTT TGG TGG CAC
	SacI-R	tcc ccgcgg CAC CCC AAT CTT CAT GTC CAC
CLTC	BglII-F	ga agatct ATG GCC CAG ATT CTG CCA ATT C
	SacI-R	tcc ccgcgg CAT GCT GTA CCC AAA GCC AGG
GPHN	XhoI-F	ccg ctcgag ATG GCG ACC GAG GGA ATG ATC
	SacI-R	tcc ccgcgg TAG CCG TCC AAT GAC CAT GAC
ICAM1	HindIII-F	ccc aagctt ATG GCT CCC AGC AGC CCC CGG
	SacI-R	tcc ccgcgg GGG AGG CGT GGC TTG TGT GTT C
ILK	XhoI-F	ctc gag ATG GAC GAC ATT TTC ACT CAG
	Sall-R	gtc gac CCC TTG TCC TGC ATC TTC TCA A
MCC	Hind3	aag ctt ATG ATG GCG GCC GCG G
	Sall-R	gtc gac CCA AGC GAA GTT TCA TTG GTG TGT GG
RPSA	XhoI-F	ctc gag ATG TCC GGA GCC CTT GAT
	Sall-R	gtc gac CCA GAC CAG TCA GTG GTT GCT C
RPSA	XhoI-F	ctc gag GGATGTCCGGAGCCCTT
	BamHI-R	gga tcc TTA A GAC CAG TCA GTG GTT GCT C
SFTP B	XhoI-F	ctc gag ATG CAC CAA GCA GGG TAC C
	Sall-R	gtc gac CAA AGG TCG GGG CTG TG

Table2. Lists of primer sequences of metastasis related cancer-associated genes

Small letters of the primer sequence indicate enzyme site and those of capital letters are the sense or antisense codon sequence of the genes.

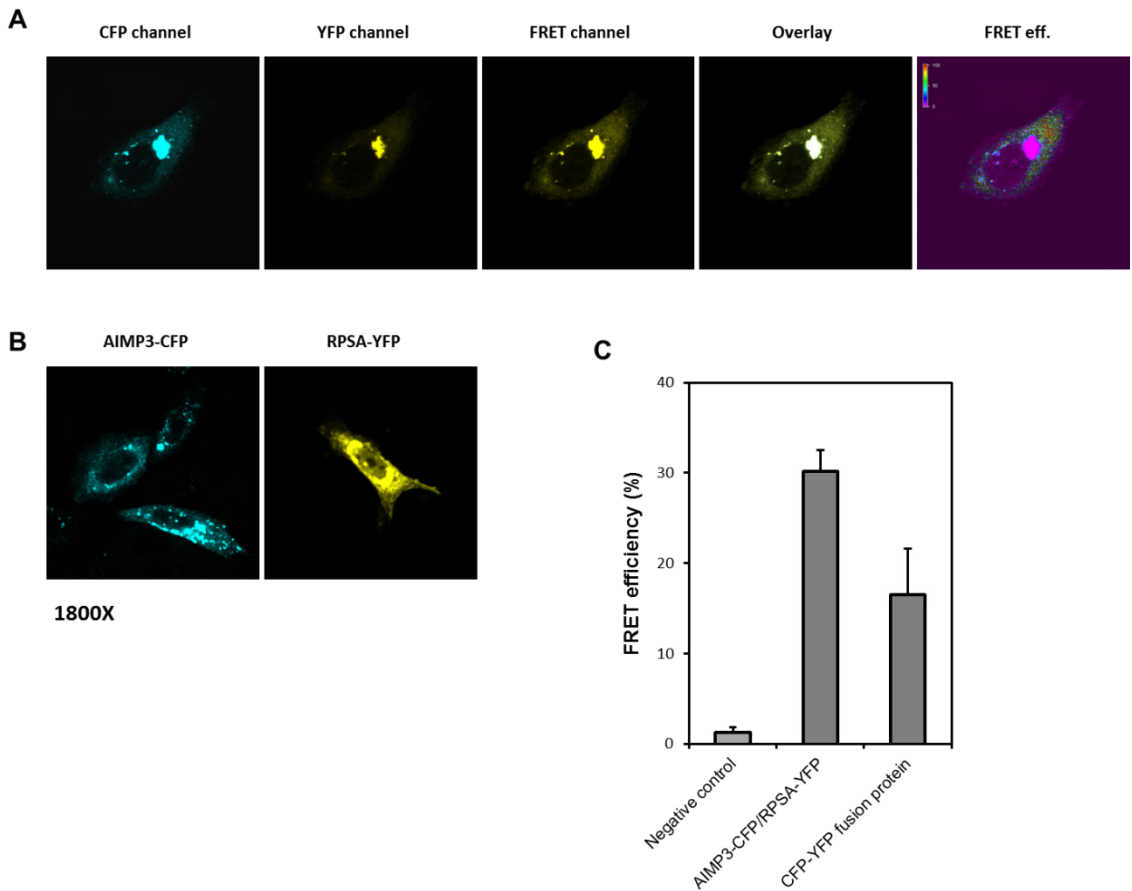


Figure2. AIMP3-CFP & RPSA-YFP pair was positive result by the FRET screening

(A) Representative confocal microscopy images of cells co-transfected with AIMP3-CFP and RPSA-YFP genes. Constructs were transfected to CHO-K1 cells. After incubate for 24 hours, confocal microscope images were taken. CFP was excited at 457nm, and its fluorescence was detected in a

wavelength of 464~499nm (CFP channel), YFP was excited at 514nm and emitted at 525~555nm (YFP channel). FRET was detected at the excitation of 457nm and the emission of 525~555nm (FRET channel). The FRET efficiency was calculated for each pixel in the image, and depicted using discrete pseudocolors. Red dots represent a higher FRET efficiency. The data show that FRET occurred in the cytosolic region of the cell. (B) CFP and YFP images in cells transfected with a plasmid encoding AIMP3-CFP or RPSA-YFP, respectively. (C) The histogram depicted the FRET efficiency from CFP to YFP in the cells transfected with negative control, both CFP-AIMP3 and YFP-RPSA, CFP-YFP fusion protein respectively. Error bars represent the s.e.m., $n=24$; Differences in the mean FRET efficiency between CFP-AIMP3, YFP-RPSA and CFP-YFP fusion protein were statistically significant at $p<0.005$, two-tailed t -test.

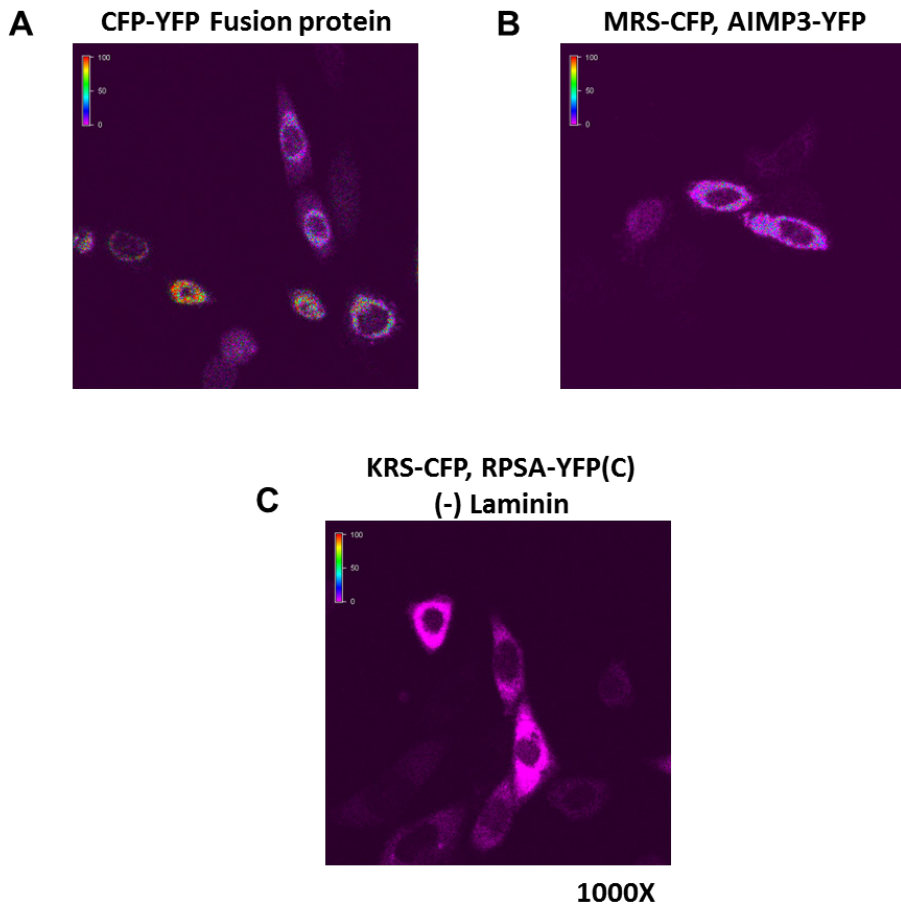


Figure3. The comparison of the FRET screening results between the positive control and negative control

The FRET efficiency was indicated using discrete pseudocolors. As shown in above figures, red dots represent a higher FRET efficiency and purple dots indicate FRET had not occurred. (A) CFP-YFP fusion protein was used as a positive control for FRET. (B) MRS-CFP/AIMP3-YFP pair is the

positive control, because of those proteins are well known to interact each other. These two data depicted that energy transfer between CFP and YFP has occurred. (C) Upon treating laminin, KRS binds to RPSA protein directly. Thus, without laminin treatment, KRS-CFP/RPSA-YFP(C; YFP tagged at C-terminal of the RPSA) pair was used as a negative control. The data as a whole consist of the purple dots.

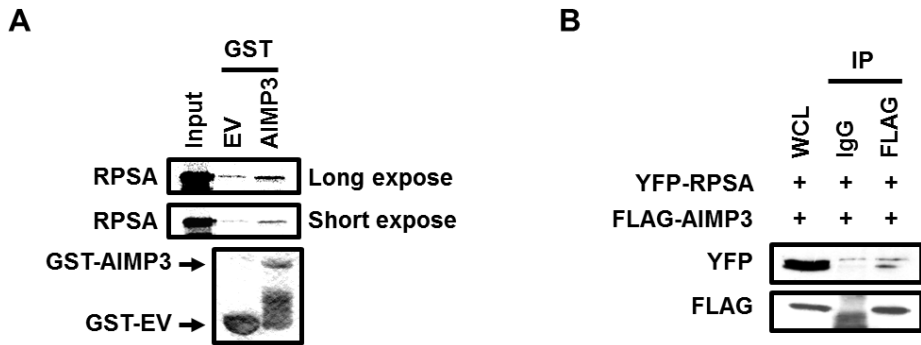


Figure4. AIMP3 physically interacts with RPSA

AIMP3 physically interacts with RPSA. (A) Upper panel: RPSA co-precipitated with GST-AIMP3 was detected by autoradiography. Lower panel: The coomassie staining represents GST and GST-AIMP3 proteins that added to radioactively synthesized RPSA. (B) Co-immunoprecipitation (Co-IP) of AIMP3 with RPSA. Lysates either from CHO-K1 cells were incubated with a FLAG antibody overnight, followed by western blot with an anti-YFP antibody. The crude lysates from these cells were used as input.

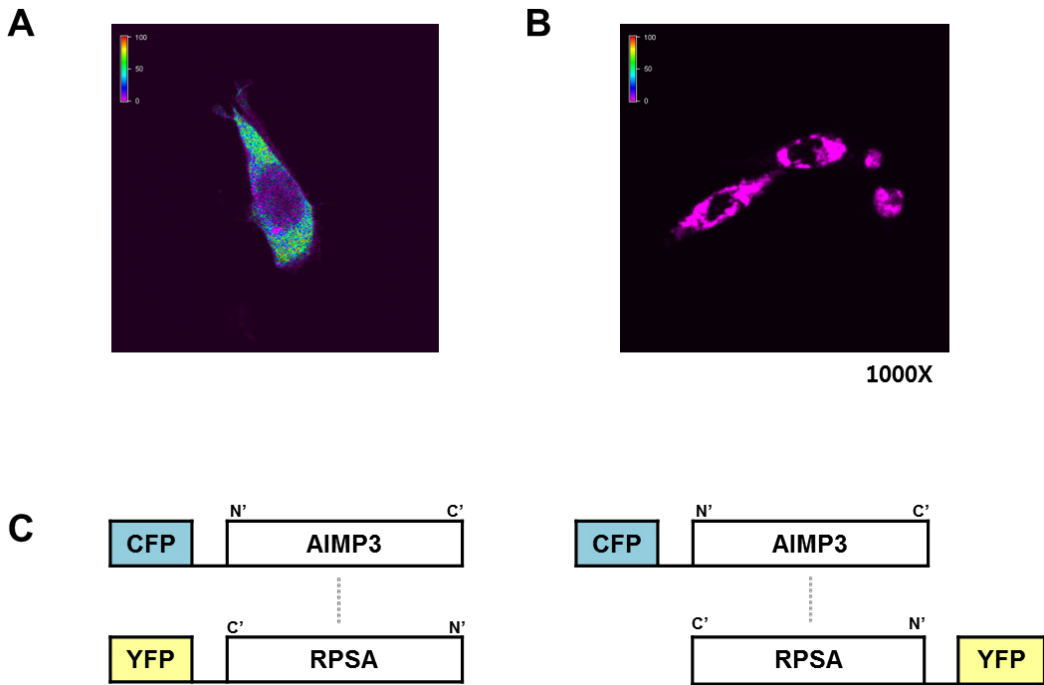


Figure 5. AIMP3 and RPSA must have the appropriate relative orientation to transfer the energy

The FRET efficiency is dependent on the relative orientation of the donor and the acceptor. The FRET efficiency images acquired from cells expressing the (A) AIMP3-CFP(N')/RPSA-YFP(C') pair and (B) AIMP3-CFP(N')/RPSA-YFP(N') pair, respectively. (C) Schematic diagrams of the relative orientation of each of pairs.

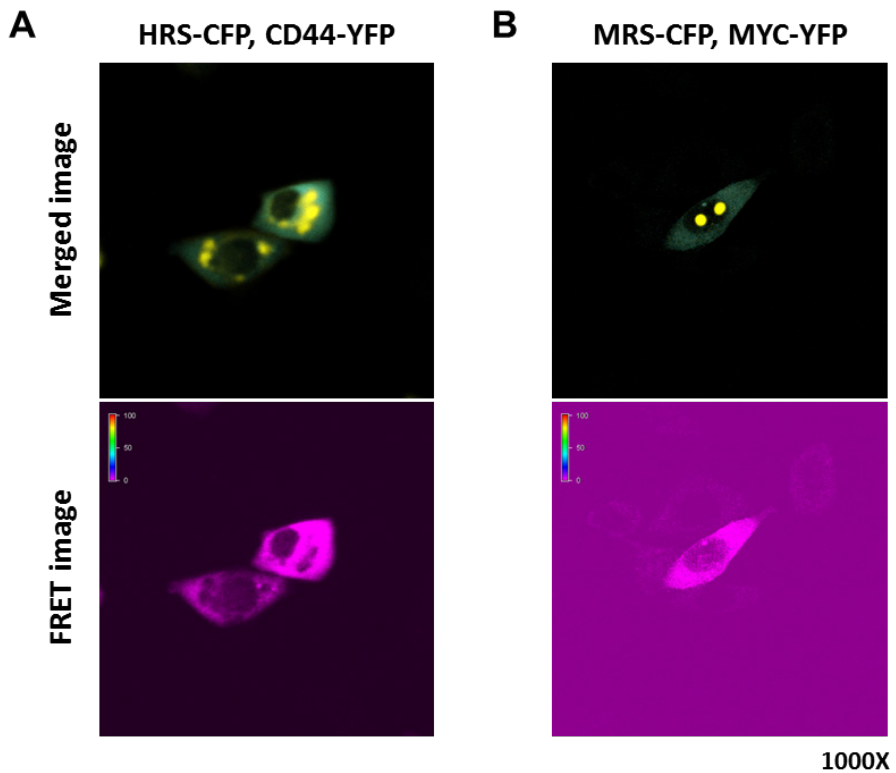


Figure6. Molecules must be in close proximity on a nanometer (10^{-9} m) scale

The FRET efficiency is influenced by the distance of the two fluorophores. The CFP and YFP have appropriate fluorescence excitation and emission properties for the measurement of close molecular distances. (A) Upper panel: The merged image from cells co-transfected with HRS-CFP and CD44-YFP shows that those two fluorescent proteins were partly coincide with the cytosolic region partly. Lower panel: However, the image of the

FRET efficiency did not show the positive results. (B) Upper panel: Unlike MRS-CFP protein expressed in cytosolic region, MYC-YFP was localized in nucleus of the cell. Lower panel: The image of the FRET efficiency from the cells expressing MRS-CFP and MYC-YFP indicates that FRET has not occurred.

DISCUSSION

We have described in this paper the development of a protein-protein interaction screening system using FRET technique. The capability of this system was demonstrated to study protein interaction between ARSs and Cancer-associated genes in the living cells. As a result, we found that the AIMP3 and RPSA pair was physically interacts each other with high FRET efficiency (Figure 2&4).

The FRET-based screening system still needs a number of steps and careful characterization to create sensitive and specific FRET pairs, such as a choice of orientation of tagged fluorescent protein efficiently (Figure 5&6). This system has contributed to our understanding of the spatiotemporal dynamics of signaling molecules in living cells, which could not be investigated using the techniques of conventional biochemistry adequately. Although FRET is mostly laborious work because of the pairs of proteins could be optimized only by trial and error, our FRET-based screening system has several merits for the screening of anticancer drugs. First, the cell-based

assay for the hit-compounds guarantees drug-delivery into the cells efficiently. Second, multiple potential drug targets in the oncogene can be screened simultaneously. Third, the time-course of the effect of drugs can also be acquired in a single experiment. That is why FRET biosensors localized to the cytoplasm, nucleus, and plasma membrane can be distinguished by an image-processing program. In the future, one can predict great utility for highly integrated cellular microarrays based on cellular FRET imaging.

REFERENCES

1. Han, J.M., J.Y. Kim, and S. Kim, *Molecular network and functional implications of macromolecular tRNA synthetase complex*. Biochemical and Biophysical Research Communications, 2003. **303**(4): p. 985-993.
2. Park, S.G., E.C. Choi, and S. Kim, *Aminoacyl-tRNA synthetase-interacting multifunctional proteins (AIMPs): a triad for cellular homeostasis*. IUBMB Life, 2010. **62**(4): p. 296-302.
3. Kim, S., S. You, and D. Hwang, *Aminoacyl-tRNA synthetases and tumorigenesis: more than housekeeping*. Nat Rev Cancer, 2011. **11**(10): p. 708-18.
4. Jares-Erijman, E.A. and T.M. Jovin, *FRET imaging*. Nat Biotechnol, 2003. **21**(11): p. 1387-95.
5. Förster, T., *Zwischenmolekulare energiewanderung und fluoreszenz*. Annalen der Physik, 1948. **437**: p. 55-77.
6. Aoki, K., et al., *Stable expression of FRET biosensors: a new light in cancer research*. Cancer Sci, 2012. **103**(4): p. 614-9.
7. Rizzo, M.A., et al., *Optimization of pairings and detection conditions for measurement of FRET between cyan and yellow fluorescent proteins*. Microsc Microanal, 2006. **12**(3): p. 238-54.

8. Elangovan, M., *Nanosecond fluorescence resonance energy transfer-fluorescence lifetime imaging microscopy to localize the protein interactions in a single living cell*. Journal of Microscopy, 2002. **205**: p. 3-14.
9. Piston, D.W. and G.J. Kremers, *Fluorescent protein FRET: the good, the bad and the ugly*. Trends Biochem Sci, 2007. **32**(9): p. 407-14.
10. Kenworthy, A.K., *Imaging protein-protein interactions using fluorescence resonance energy transfer microscopy*. Methods, 2001. **24**(3): p. 289-96.
11. Komatsu, N., et al., *Development of an optimized backbone of FRET biosensors for kinases and GTPases*. Mol Biol Cell, 2011. **22**(23): p. 4647-56.
12. Shaner, N.C., P.A. Steinbach, and R.Y. Tsien, *A guide to choosing fluorescent proteins*. Nat Methods, 2005. **2**(12): p. 905-9.
13. Rizzo, M.A., et al., *An improved cyan fluorescent protein variant useful for FRET*. Nat Biotechnol, 2004. **22**(4): p. 445-9.
14. Cantera, J.L., W. Chen, and M.V. Yates, *A fluorescence resonance energy transfer-based fluorometer assay for screening anti-coxsackievirus B3 compounds*. J Virol Methods, 2011. **171**(1): p. 176-82.
15. Kim, J., et al., *Quantification of protein interaction in living cells by two-photon spectral imaging with fluorescent protein fluorescence resonance energy transfer pair devoid of acceptor bleed-through*. Cytometry A, 2012. **81**(2): p. 112-9.

16. Kwon, N.H., et al., *Dual role of methionyl-tRNA synthetase in the regulation of translation and tumor suppressor activity of aminoacyl-tRNA synthetase-interacting multifunctional protein-3*. Proc Natl Acad Sci U S A, 2011. **108**(49): p. 19635-40.
17. Kim, D.G., et al., *Interaction of two translational components, lysyl-tRNA synthetase and p40/37LRP, in plasma membrane promotes laminin-dependent cell migration*. FASEB J, 2012. **26**(10): p. 4142-59.
18. Miyawaki, A., *Visualization of the Spatial and Temporal Dynamics of Intracellular Signaling*. Developmental Cell, 2003. **4**: p. 295-305.

국문 초록

Aminoacyl-tRNA synthetases (ARSs)는 단백질 합성과정 중 tRNA에 상보적인 아미노산을 결합시켜주는 필수효소로서 세포의 생존에 관여한다. 그러나 이전의 연구에 따르면 일부 ARS의 발현은 cellular type과 stress 상황에 따라 변하며 다양한 세포 내 반응에 관여한다는 것이 밝혀졌다. 또한 최근 bioinformatics를 기반으로 한 연구 결과에서 23개의 aminoacyl-tRNA synthetases (ARSs)와 123개의 cancer-associated factor가 밀접한 관련이 있는 것으로 보고되었기 때문에 이 두 가지 단백질들 간의 상관관계를 밝히는 assay의 필요성이 대두되었다. 따라서 본 연구에서는 fluorescence resonance energy transfer (FRET) technique을 사용하여 ARSs와 cancer metastasis와 관련된 CAG간의 tumorigenesis에 대한 상관관계를 밝혀내고자 하였다. 결과적으로 FRET 기반의 screening system을 사용하여 AIMP3와 RPSA 단백질간의 상호작용이 있음을 확인하였고, co-immunoprecipitation과 in vitro pull down assay를 통해 직접적으로 결합하고 있음을 증명했다.

주요어: Aminoacyl-tRNA synthetases (ARSs), Cancer-associated genes (CAGs), protein-protein interaction, Fluorescence resonance energy transfer (FRET), anti-

cancer drug target

학번: 2011-23058